

Relaxation of stored charge carriers in a $\text{Zn}_{0.3}\text{Cd}_{0.7}\text{Se}$ mixed crystal

J. Y. Lin and H. X. Jiang

Department of Physics, Kansas State University, Cardwell Hall, Manhattan, Kansas 66506-2601

(Received 28 September 1989)

Persistent photoconductivity (PPC) has been investigated in detail in a $\text{Zn}_{0.3}\text{Cd}_{0.7}\text{Se}$ mixed crystal. Two different temperature conductivity states have been observed. Relaxation of stored charge carriers, which contribute to PPC, has been studied at different conditions. We find that the decay of PPC follows the "stretched-exponential" function that is usually observed in a wide class of disordered materials. At $T < 220$ K, the relaxation time increases with increase of temperature. At a constant temperature, the relaxation time increases with increase of excitation photon dose, which is a consequence of the presence of the two different conductivity states. However, at a constant temperature, the decay exponent is excitation-photon-dose independent, while the characteristic decay time constant depends on excitation photon dose. The PPC observed here thus exhibits characteristic phenomena of disordered systems, which suggests that the random local-potential fluctuations, which arise from the compositional fluctuations, are responsible for PPC. PPC-decay behavior is also analyzed for some of the previously published data on other materials. We find that the stretched-exponential function describes the PPC decay in various materials at low temperatures.

I. INTRODUCTION

Persistent photoconductivity (PPC), photoconductivity that persists after the removal of the photoexcitation, has recently attracted renewed attention. PPC has been observed in a wide variety of semiconducting materials,¹ reported in III-V compounds such as $\text{Al}_x\text{Ga}_{1-x}\text{As}$ (Refs. 2-6) and in artificially constructed layered materials⁷⁻⁹ at low temperatures. Recently, PPC has been discovered in doping-modulated amorphous-silicon superlattices,¹⁰⁻¹² in undoped II-VI mixed crystals,^{13,14} and has been shown to exist even at room temperatures. PPC is very important from the point of view of device performance because it is detrimental to the operation of modulation-doped field-effect transistors (MODFET's) at low temperatures.¹⁵ However, PPC is useful for adjusting the density of the two-dimensional electron gas at a semiconductor interface,¹⁶ and can be utilized as a nondestructive method to probe the profile of the impurities in semiconductors.¹⁷ Other applications of PPC include optoelectronic memory elements, vidicons, etc.¹ Discovery of the room-temperature PPC phenomena makes the PPC-based devices feasible. In fundamental physics, understanding of PPC phenomena will provide mechanisms for basic physical processes in semiconductors such as charge-carrier excitation, transformation, storage, and relaxation. Thus PPC is one of the most important yet not-well-understood phenomena in semiconductors.

Several mechanisms have been proposed to explain the origin of PPC. Queisser and Theodorou have demonstrated for well-defined heterostructural samples that the spatial separation of photogenerated electrons and holes by built-in electric field from macroscopic barrier due to band bending at surfaces or interfaces leads to PPC.⁸ For layered structures of compound semiconductors, this model predicts an essentially logarithmic PPC decay in time consistent with their experimental observation.

However, this model is only suitable to describe PPC in artificially constructed layered materials. The PPC decay mechanism for bulk semiconductors cannot be described in terms of the macroscopic barrier model. The other dominant mechanism involves photoexcitation of electrons from deep level traps which undergo a large lattice relaxation, namely, DX centers.^{3,4} In this model, PPC has resulted because recapture of electrons by DX centers is prevented by a thermal barrier at low temperatures. The large lattice relaxation model explains the large Stokes shift of ≈ 1 eV between the thermal and optical ionization energies observed in $\text{Al}_x\text{Ga}_{1-x}\text{As}$. The photo-capacitance results obtained for Si-doped GaAs under pressure were found to be very similar to the results observed for $\text{Al}_x\text{Ga}_{1-x}\text{As}$ alloys at atmospheric pressure,¹⁸⁻²⁰ and thus favor the large lattice relaxation model. The nature of the DX center is under intensive investigation. Recently, Chadi and Chang performed pseudopotential calculations to determine the atomic displacements responsible for the formation of DX centers in Si- and S-doped GaAs. Their results indicate that DX is a highly localized and negatively charged defect center which behaves as a negative- U center resulting from the "reaction" $2d^0 \rightarrow d^+ + (DX)^-$, where d represents a substitutional donor.^{21,22} Although the DX center in $\text{Al}_x\text{Ga}_{1-x}\text{As}$ alloys exhibits a PPC effect, conclusions derived from the negative- U model are not consistent with existing Hall experiments for Si-doped $\text{Al}_x\text{Ga}_{1-x}\text{As}$. Recently, Li *et al.* pointed out that the discrepancy between the negative- U model and Hall experiments can be improved if there exists two different donors SD and DX with comparable concentrations,²³ where SD centers provide electrons for DX centers to capture. However, the origin of SD is not clear. Furthermore, recent magnetic studies of PPC in n -type $\text{Al}_x\text{Ga}_{1-x}\text{As}$ by Khachatryan *et al.*²⁴ concluded that the DX center is a paramagnetic donor with one unpaired electron. Thus the nature of the

DX center is very complicated and the origin of PPC in $Al_xGa_{1-x}As$ materials is not yet completely understood. Additionally, because of the complex nature of the *DX* center, the decay behavior of PPC exhibited by these materials has not yet been established.²⁵⁻²⁷ Obviously, the decay kinetics are very important in determining the origin for the slow relaxation of the photoexcited charge carriers. Zukotynski and Ng suggested an alternative explanation for PPC observed in Si-doped $Al_xGa_{1-x}As$, in which PPC is caused by periodic fluctuations in As versus Ga concentration which lead the shift of the impurity wave function in *k* space.²⁸ However, periodic fluctuations are not expected in a real space. More realistically, the composition fluctuations in mixed crystals are random.

PPC has been briefly investigated in undoped $Zn_xCd_{1-x}Se$ mixed crystals recently in our earlier work.¹³ A PPC related phase transition has been observed at T_C (≈ 120 K) for $Zn_{0.3}Cd_{0.7}Se$ mixed crystal, which corresponds to electrons activated from localized-to percolation-state regions. Additionally, we found that PPC is not observable at temperatures below 70 K, and shows stretched-exponential decay behavior. The percolation features show evidence that random local-potential fluctuations shown schematically in Fig. 1, which arise from the compositional fluctuations, are the origin of PPC observed in II-VI mixed crystals. The microscopic random-potential fluctuation model was frequently used to describe charge-transport properties of strongly compensated, inhomogeneous, and amorphous semiconductors.^{29,30} According to this model description, the Fermi level falls in the localized region, and the charge transport occurs either via activated electron hopping between localized states or by activation of electrons into the percolation-state region, while holes remain localized. Therefore, a transition from localized to delocalized states is expected from this model. Additionally, the electron states are highly localized at lowest tempera-

tures, and the charge transport becomes negligible. The PPC behavior exhibited by $Zn_xCd_{1-x}Se$ mixed crystals is consistent with the results which are expected from the random local-potential fluctuation model. To our knowledge, a quantitative understanding and conclusive experiments on such systems have never been achieved previously. In mixed crystals, large compositional fluctuations are well known,³¹⁻³³ which causes local-potential fluctuations in the sample. Thus mixed crystals represent a whole new system of percolative semiconductors, and can serve as a model system for the study of the carrier transport in percolative solids. The quantitative understanding of the relaxation process of stored charge carriers will also provide model description for other fundamental relaxation processes, such as spin relaxation of spin glasses, etc.

In this paper, PPC phenomena in $Zn_{0.3}Cd_{0.7}Se$ are investigated in more details. In Sec. II, we describe the experimental techniques. In Sec. III, dependencies of PPC on temperature and photon dose are presented, and the decay behavior is studied at different conditions. In Sec. IV, by using previously published experimental data, decay behavior is studied for various semiconducting systems and configurations. The similarity between the relaxation processes of charge carriers in II-VI mixed crystals and various other materials has been discussed. The stretched-exponential decay behavior exhibited by different materials at low temperatures suggests that the local-potential fluctuations may be an additional cause for PPC observed in other materials.

II. EXPERIMENT

The sample used in this study is a 1-mm-thick $Zn_{0.3}Cd_{0.7}Se$ mixed crystal of size about $5\text{ mm} \times 10\text{ mm}$ with dark room-temperature resistivity of about $10^9\ \Omega\text{ cm}$. Single crystal were grown from solid solution. The starting materials were purified ZnSe and CdSe powders in appropriate weight proportions. Crystals were grown by using the temperature-gradient solution-zoning technique. $Zn_xCd_{1-x}Se$ mixed crystals with $0 \leq x \leq 0.4$ were of hexagonal structure.³⁴ Gold leads were attached to the sample using indium solder and the junctions of 1 mm in diameter were about 5 mm apart on the sample surface and carefully tested for Ohmic contacts. The optic *c*-axis is perpendicular to the sample surface. The sample was attached to a copper sample holder, which is inside a closed-cycle He refrigerator, with care taken to ensure good thermal contact yet electrical isolation. A mercury lamp was used along with appropriate filters, so two lines at 435.8 and 546.1 nm dominated the output of the excitation source. The data obtained at different conditions were taken in such a way that the system was always allowed to warm up to the room temperature and relaxed to equilibrium after each measurement, then cooled down in darkness to the desired temperature of measurements. This is to ensure that each set of data has the same initial condition. Additionally, the temperature-dependent PPC-decay behavior is obtained by illuminating the sample by exactly the same amount of photon dose at every temperature of decay measure-

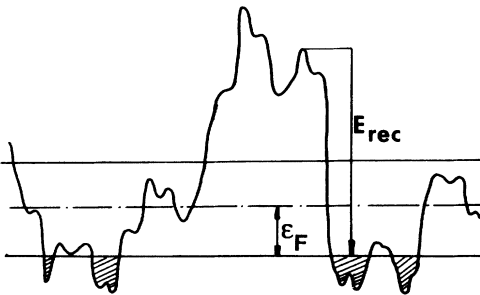


FIG. 1. Schematic of the conduction-energy diagram of a random-potential profile of a disordered semiconductor. The meandering line shows band bending. The upper solid line indicates the position of the bottom of the conduction band in the absence of the local-potential fluctuations, which arise from either the compositional fluctuations or the impurity potential. Each lower solid line shows the electron Fermi level, the dashed-dotted line the percolation level. Regions occupied by electrons are shaded (after B. I. Shklovskii and A. L. Efros, Ref. 39).

ments. The low excitation level is used to ensure that no photoconductivity (PC) is induced at the low-temperature regions. This can be achieved because the PC level depends only on excitation light intensity, which is in contrast to the PPC property. The PPC buildup level depends on excitation photon dose. The typical excitation photon flux used for the measurements is about 2×10^{13} photons/cm²s. The current is measured by a Keithley digital electrometer (model 617). A 1.5-V bias is supplied by a battery.

III. RESULTS AND DISCUSSIONS

For the Zn_{0.3}Cd_{0.7}Se crystal, temperature-dependent results yield four different regions. For $T < 70$ K, virtually no PPC could be observed. In the temperature region of $70 \text{ K} < T < 120 \text{ K}$, illumination induces low-level PPC. In the region $125 \text{ K} < T < 220 \text{ K}$, the same level of light excitation produces a pronounced PPC effect. As the temperature becomes above 220 K, the same level of photoexcitation induces PC and PPC simultaneously.

Figure 2 shows decay curves obtained at 170 K for four different excitation intensities at 1000 sec of light illumination. The experimental data are normalized to the current value at $t=0$, and the dark equilibrium current value has been subtracted out. In general, at a constant temperature, prior the conductance reaching saturation, relaxation of PPC proceeds faster with decrease of the illumination photon dose, as depicted in Fig. 2. We see that the PPC relaxation proceeds fastest for the relative photon dose $n=0.8$, and slowest for the relative photon dose $n=4.0$. The units of photon dose are 10^{16} photons/cm². Changing the illumination time at a constant photoexcitation intensity by identical factors produces a similar behavior, which implies that PPC depends on excitation photon dose but not only on intensi-

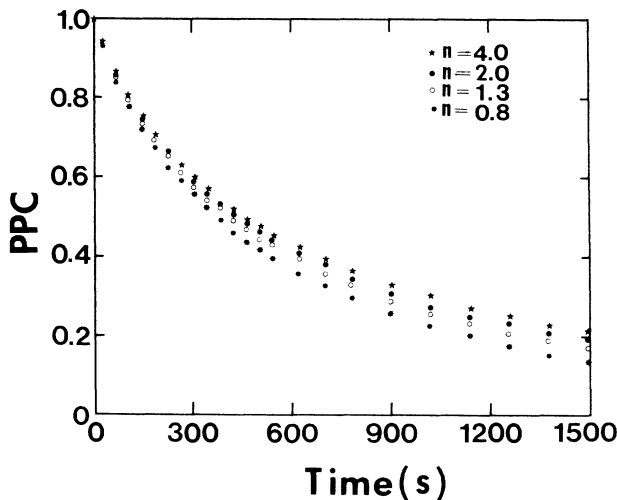


FIG. 2. PPC decay obtained at 170 K after buildup with four different excitation intensities for 1000 s. Each curve is normalized to a unity at $t=0$, and the dark current has been subtracted out. The unit for excitation photon dose n indicated in the figure is 10^{16} photons/cm².

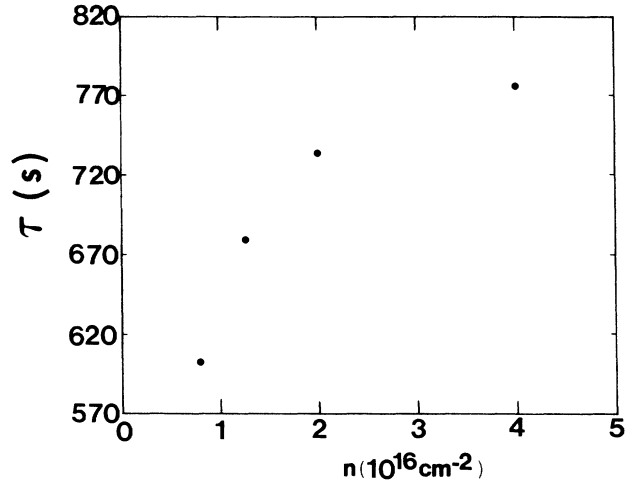


FIG. 3. The characteristic decay-time constant τ as a function of excitation photon dose at $T=170$ K.

ty. At temperatures $T < 220$ K, the decay of PPC can be well described by the “stretched-exponential” function,¹³ $I_{\text{PPC}}(t) = I_{\text{PPC}}(0) \exp[-(t/\tau)^\beta]$, where β ($0 < \beta < 1$) is the decay exponent and τ is the characteristic decay time constant. τ increases with increase of excitation photon dose. At 170 K, τ as a function of excitation photon dose is presented in Fig. 3, where a strong dependence of the relaxation time on excitation photon dose is evident. However, β is independent of excitation photon dose at a constant temperature, $T=170$ K. This property is clearly demonstrated by the scaling effect. Figure 2 is replotted in Fig. 4 in such a way that the time of each curve has been scaled by the corresponding value of τ in Fig. 3, so the decay behavior of PPC can be written as

$$I_{\text{PPC}}(t') = I(0) \exp[-(t')^\beta], \quad 0 < \beta < 1, \quad (1)$$

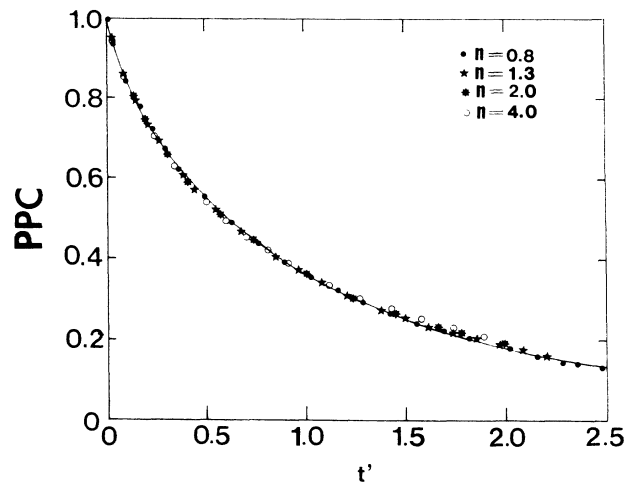


FIG. 4. Scaled decay curves obtained at 170 K. t' ($\equiv t/\tau$) is the dimensionless scaled time, where the scale factors used are the corresponding values of the characteristic decay-time constants τ from Fig. 3. The solid line is a plot of the stretched-exponential function $I(t') = I(0) \exp[-(t')^\beta]$, with $\beta=0.77$.

where the scaled time $t' = t/\tau$, and τ is the characteristic decay time constant obtained for different excitation photon dose taken from Fig. 3. The striking feature shown in Fig. 4 is that the rescaled PPC-decay curves obtained at different excitation photon dose fit perfectly to a single stretched-exponential function of Eq. (1) with $\beta = 0.77$. In Fig. 4, the solid line is a plot of a stretched-exponential function, $I(t') = I(0)\exp[-(t')^\beta]$, with $\beta = 0.77$. Thus properties of PPC decay following the stretched-exponential and the decay parameter β being independent of excitation photon dose are demonstrated.

The stretched-exponential decay frequently describes the relaxation of a wide class of disordered systems toward equilibrium.³⁵ Examples include dielectric relaxation in a charged-density-wave system³⁶ and relaxation of remanent magnetization in spin glasses.³⁷ Recently, Kakalios, Street, and Jackson observed stretched-exponential relaxation for density of shallow occupied band-tail states of hydrogenated amorphous silicon.³⁸ A class of models was proposed based on *hierarchically constrained dynamics*, from which the stretched-exponential relaxation arises naturally.³⁹ Thus the PPC-decay behavior reveals the similarity of the present system to the disordered systems. For mixed crystals, the stretched-exponential relaxation of photoexcited charge carriers is a consequence of the compositional disorder effect. The results suggest that the random local-potential fluctuations, which arise from the compositional fluctuations in the sample, are responsible for PPC. A schematic diagram of the random local-potential fluctuations at the conduction-band edge is shown in Fig. 1. In this model description, the photoexcited charge-carrier density is highly inhomogeneous. Spatially, electrons fall into localized regions, which form due to the variations in composition or variations in band gap from one state to another. At lower temperatures, conductivity is contributed by the electron hopping between localized states (potential wells). As temperature increases to above a critical value, T_C , electrons can be activated into percolation states, which requires a thermal energy in the order of ϵ_F shown in Fig. 1. In the percolation states, the transport occurs via electrons percolating through the network of accessible states. The relaxation rates in the above-mentioned two conductivity states are determined by the charge-carrier distribution, i.e., the wave-function overlap between the electrons and the holes in the real space. A further increase in temperature results in electrons overcoming the potential barrier of height E_{rec} , and the photoexcited charge carriers recombine very quickly. The percolation approach thus no longer describes well the conductivity mechanism at high temperatures ($T > 220$ K).

Experimentally, the PPC effect exhibited by $\text{Zn}_{0.3}\text{Cd}_{0.7}\text{Se}$ mixed crystal is consistent with the random local-potential fluctuation model. The inset of Fig. 5 shows the PPC buildup level as a function of temperature for 1000 sec of light illumination at an excitation intensity of about 2×10^{13} photons/cm². In the temperature region $70 \text{ K} < T < 120 \text{ K}$, the Fermi level falls in the localized region, and the system is in the low conductivity state, in which case PPC is contributed by activated elec-

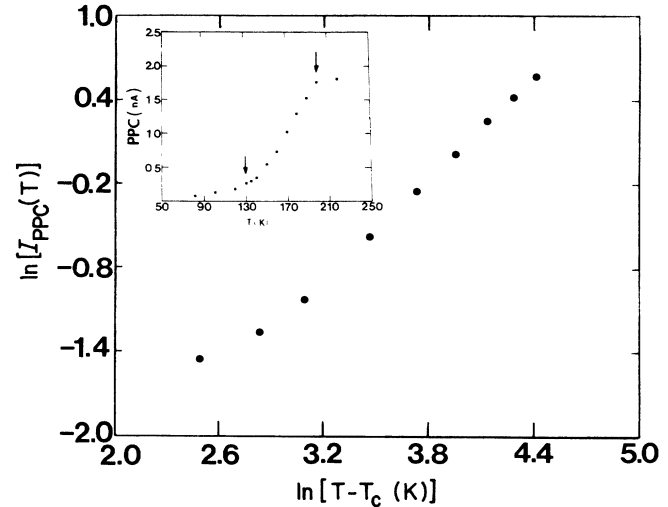


FIG. 5. Plot of $\ln[I_{\text{PPC}}(T, t=0)]$ vs $\ln(T - T_c)$ with $T_c = 118 \pm 2$ K at an excitation intensity of 2×10^{13} photons/cm²s with 1000 s of light illumination. The slope of the linear curve represents the conductivity exponent ν ($= 1.30 \pm 0.05$). The inset shows the linear plot of the PPC buildup level at $t=0$, $I_{\text{PPC}}(T, t=0)$, vs temperature. Two arrows indicate the temperature region for $\ln[I_{\text{PPC}}(T, t=0)]$ vs $\ln(T - T_c)$ plot.

tron hopping between localized states. However, a large increase in PPC is observed near 120 K. This is a consequence of the electrons activated from localized to delocalized (percolation) states. At temperatures above 120 K, PPC is predominantly contributed by percolation conductance, while the holes still remain localized (the effective mass of the holes is much larger than that of the electrons). Thus at temperatures above the percolation threshold, we expect that the temperature-dependent PPC buildup level shown in the inset of Fig. 5 can be described by the percolation approach:

$$I_{\text{PPC}}(T) = \alpha(T - T_c)^\nu \quad T > T_c, \quad (2)$$

where ν is the conductivity exponent. Least-squares fitting between experimental data and Eq. (2) in the temperature region $130 \text{ K} < T < 200 \text{ K}$ yields the results that the conductivity exponent $\nu = 1.30 \pm 0.05$ and the critical temperature $T_c = 118 \pm 2$ K. In Fig. 5 we plot $\ln[I_{\text{PPC}}(T)]$ versus $\ln(T - T_c)$ for the experimental data obtained in the region $130 \text{ K} < T < 200 \text{ K}$. The linear behavior indicates that the PPC buildup level is well described by Eq. (2). However, one notices that the fit becomes poorer near the percolation threshold, which is expected from the percolation behavior. Near the percolation threshold, an additional contribution from electron hopping elevates the PPC level. The fitting thus curves away from Eq. (2) at temperatures near the threshold. This behavior has been observed previously for many other materials.⁴⁰ We also fit $I_{\text{PPC}}(T)$ in the same region with an exponential dependence, $I_{\text{PPC}}(T) = \alpha \exp(-E/kT)$, and the fit is not as good as the percolation approach. The decay behavior of PPC and the

phase transition in PPC near 120 K support our interpretation that PPC is induced by the random local-potential fluctuations in the sample. The observation of the phase transition in PPC here cannot be explained either by the large lattice relaxation model or the macroscopic barrier model.

The decay parameters β and τ are functions of temperature.¹³ The value of β is about 0.85 ± 0.03 below 120 K, and depicts a clear decrease near 120 K. The characteristic decay time constant τ also shows an increase near 120 K. Therefore, experimental results indicate that the PPC relaxation proceeds faster in the low conductivity state (hopping states). Furthermore, at $T_C < T < 220$ K, τ increases with increase of temperature, which again cannot be explained in terms of the DX or the macroscopic barrier models since these two models lead to the results that the PPC relaxation proceeds faster as the temperature increases in the entire temperature region. The relaxation behavior can only be explained in terms of the random local-potential fluctuation model. Qualitatively, we can explain the temperature-dependent decay behavior as follows: The decay of PPC depends on the distribution of charge carriers and the conductivity states. For $T < T_C$, since PPC is contributed by the electron-activated hopping between localized states, the effect of the electron redistribution among the localized states with time is negligible. Thus the decay is only determined by the initial distribution of charge carriers, and the decay rate depends on the wave-function overlap between electrons and holes. Thus the recombination kinetics in this temperature region should be similar to those of the donor-acceptor pair recombination.⁴¹⁻⁴³ At $T > T_C$, electrons activated into the percolation states, the effect of electron redistribution in real and momentum spaces, plays an important role. Electrons redistribute in such a way that they always prefer to occupy the sites of minimum potential energies. In the percolation description, conductivity is contributed by electrons percolating through the network of accessible sites (locations of low potential energy). The time duration of an electron on each accessible site depends on the potential depth of the site and thus depends on the composition x at each site. It is easy to understand that the probability for finding an electron at the site of minimum potential is highest compared to other sites, because, relatively, electrons tend to spend more time on such site. Since holes remain localized and immobile, the recombination becomes spatially less possible with increase of time because of the lack of holes around these sites (nearby holes have been recombined with electrons in earlier time stages). As temperature increases, the redistribution effect becomes more pronounced, thus an increase in τ is observed. As temperature increases to above 220 K, the decay rate then increases with an increase of temperature.

The correlation between the critical temperature T_C and the degree of the fluctuation can be established. For mixed crystals $A_x B_{1-x} C$, the compositions at the spatial sites fluctuate around the mean composition x_0 . Since the sample growth is a random process, we can assume that the probability of the spatial sites with the composition x follows a Gaussian distribution,⁴⁴

$$P(x) = P_0 \exp[-(x - x_0)^2 / 2\sigma^2], \quad (3)$$

where x_0 is the mean composition. For our sample $Zn_{0.3}Cd_{0.7}Se$, x_0 is 0.3. P_0 can be determined from the normalization condition

$$\int_0^1 P(x) dx = 1, \quad (4)$$

which gives

$$P_0 = \left[\int_0^1 \exp[-(x - x_0)^2 / 2\sigma^2] dx \right]^{-1}. \quad (5)$$

σ is a parameter which describes the degree of the fluctuation in the sample, and depends on the sample quality. In order to establish the relation between σ and T_C , we assume that all the low-potential sites ($x \leq x_C$) are filled by the electrons. The transition occurs when the ratio of the filled low-potential sites to the total available sites approaches to a value, P_C , the critical concentration. This means that we have

$$\int_0^{x_C} P_0 \exp[-(x - x_0)^2 / 2\sigma^2] dx = P_C. \quad (6)$$

The value of the critical electron filling states P_C obtained from the computer simulation on three-dimensional lattices is about 0.25.⁴⁵ Therefore, Eq. (6) determines the critical composition, x_C , which stands for that all the spatial sites with composition $x \leq x_C$ are filled by the electrons. The average potential energy for the electrons filled up to sites with $x \leq x_C$ can be written as

$$\bar{V} = \frac{\int_0^{x_C} V(x) P(x) dx}{\int_0^{x_C} P(x) dx}, \quad (7)$$

where $V(x)$ is the electron energy at the conduction-band edge as a function of the composition x . For $Zn_x Cd_{1-x} Se$ mixed crystal, it is known that the band gap varies linearly⁴⁶ with x from 1.84 eV ($x=0$, CdSe) to 2.8 eV ($x=1$, ZnSe),⁴⁷ and so the energy-gap difference ΔE_g is 0.96 eV. Therefore, we have

$$V(x) = V_0 + \alpha x, \quad (8)$$

with $V_0 = 1.84$ eV and $\alpha = 0.96$ eV. Inserting Eq. (8) into Eq. (7), we obtain

$$\bar{V} = (V_0 + \alpha x_0) + \frac{\alpha P_0}{P_C} \sigma^2 \{ \exp(-x_0^2 / 2\sigma^2) - \exp[-(x_C - x_0)^2 / 2\sigma^2] \}. \quad (9)$$

The transition occurs if the averaged total energy of an electron equals the energy at the percolation threshold $V(x_C)$. Thus we obtain

$$\bar{V} + \frac{3}{2} k T_C = V(x_C), \quad (10)$$

where $(\frac{3}{2})kT_C$ is the average thermal energy of an electron. Therefore, from Eqs. (9) and (10), we have

$$T_C = \frac{2}{3k} \alpha (x_C - x_0) - \frac{2\alpha P_0 \sigma^2}{3k P_C} \left\{ \exp(-x_0^2/2\sigma^2) - \exp[-(x_C - x_0)^2/2\sigma^2] \right\}. \quad (11)$$

Equation (11) has been calculated numerically and the critical temperature T_C is obtained as a function of the fluctuation parameter σ . From $T_C = 118$ K, obtained from the experimental measurement for $\text{Zn}_{0.3}\text{Cd}_{0.7}\text{Se}$, we find $\sigma = 0.027$. This is a reasonable value for the fluctuation in the sample. However, in the calculation, we have used a band offset of 100% for the conduction band, and the valence-band offset was not considered. The calculated σ should be lower than the actual value. If we consider the band offset, the expression for α in Eqs. (8)–(11) should be replaced by $\alpha \cdot \Delta Q_C$, where $\Delta Q_C (= \Delta E_C / \Delta E_g)$ is the conduction-band offset, and ΔE_C is conduction-band energy difference between the two materials. By taking ΔQ_C to be 80%, we obtain a σ value to be 0.033. In the above calculation, the electron distribution in momentum space has been neglected. However, the results obtained by including such a term should not deviate from the present calculation by a significant factor.

The results shown in Fig. 2 can be qualitatively interpreted in terms of the variation of the electron Fermi-energy level with excitation photon dose. For lower photon dose, i.e., lower electron concentration, the Fermi level falls deeper into the localized states, and the conductivity is affected more pronouncedly by mean of an activation hopping process. As the electron concentration increases, the Fermi level also increases, and the effect of the activation hopping to the decay process becomes smaller. Since the PPC relaxation proceeds more slowly in the percolation states, the photon-dose-dependent PPC decay is a consequence of the different conductivity states' effect. Higher charge-carrier density leads to a more pronounced redistribution effect, thus a slower decay process. The dependence of τ on the excitation photon dose, n , can implicitly provide us information on the dependence of the charge-carrier relaxation on the Fermi level. We have experimentally demonstrated that, at a constant temperature, the dependence of τ on n can be described by the following expression:

$$\tau = a + b/n, \quad (12)$$

where a and b are constants, and n is the excitation photon dose. In Fig. 6, we replot the data in Fig. 2 according to Eq. (12), τ versus $1/n$, which shows a perfect linear behavior. From Fig. 6, we obtain that $a = 820$ s and $b = -1.74 \times 10^{-14}$ s/cm². A more fundamental relationship between τ and E_F , the Fermi energy of the electron, should exist. E_F depends on the excitation photon dose n . However, the relation between E_F and n is not yet established at this stage. From Fig. 6, we see that if we extrapolate to n approaching infinite, the maximum value of τ which can be obtained at 170 K is about 820 s. The relation between τ and n should be deviated from Eq. (12) for small values of n ($n \rightarrow 0$) because τ is always a posi-

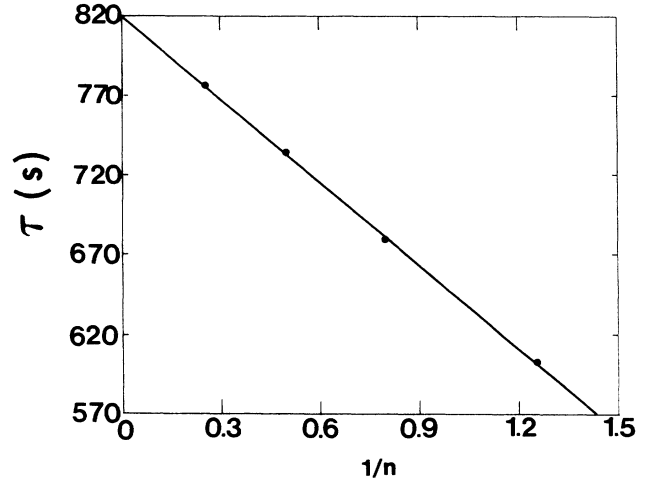


FIG. 6. Plot of the characteristic decay-time constant τ vs $1/n$, where n represents the excitation photon dose. The solid line is a guide to the eyes.

tive value. The exact dependence of τ on n for small values of n is under further investigation experimentally and also theoretically.

At temperatures $T > 220$ K, the relaxation of PPC proceeds faster as temperature increases, and the decay is no longer well described by a single stretched-exponential function. Figure 7 shows a normalized decay curve obtained at 293 K for 1000 s of light illumination. We see that the same level excitation photon dose induces PC and PPC simultaneously, and the conductance is about 10% of its initial level after 1000 s of decay time even at room temperatures. The PPC decay as illustrated in Fig. 7 has two components, and the decay can be described by an initial rapid decay followed by a stretched-exponential decay. In the description of the random local-potential fluctuation model, at higher temperatures ($T > 220$ K),

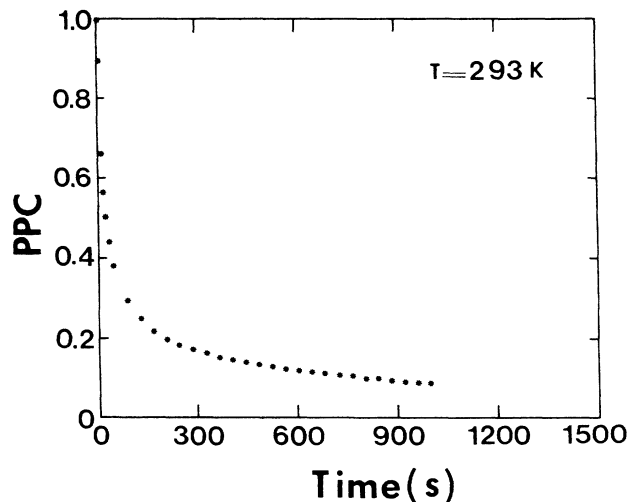


FIG. 7. Normalized decay curve obtained at 293 K for 1000 s of light illumination. The excitation intensity used is about 2×10^{13} photons/cm²s. The current value at $t = 0$ is 3.66 nA.

the thermal energy is sufficiently high so that some electrons can be transferred to the maximum of barrier height, E_{rec} , to recombine with holes soon after photoexcitation, which contribute to the PC part. The slow relaxation part corresponds to tail states contributing to PPC. Fitting data from 320 to 1000 s with the stretched-exponential decay yield the results that $\tau=107$ s and $\beta=0.32$. To date, there is no reported results on any other materials which exhibit well-characterized PPC at room temperatures. We believe that, for mixed crystals with large compositional fluctuations, well-characterized PPC should be observed at room temperatures, which is of technological importance because such an effect can be easily utilized.

IV. COMPARISON TO OTHER MATERIALS

Presently, it is widely accepted that the DX center which undergoes a large lattice relaxation is the origin of PPC observed in $\text{Al}_x\text{Ga}_{1-x}\text{As}/\text{GaAs}$ materials. It was suggested that at least two mechanisms are responsible for PPC observed in the $\text{Al}_x\text{As}_{1-x}\text{As}$ system,^{48,49} namely the presence of the DX centers, and the charge separation at the barrier. By removing the junction-causing GaAs substrate, Collins, *et al.* attempted to distinguish between the DX and the macroscopic barrier models.⁵⁰ However, they found that the PPC is due primarily to charge separation at the $\text{Al}_x\text{Ga}_{1-x}\text{As}/\text{GaAs}$ heterojunctions. A PPC effect is also observed previously in doping-modulated amorphous silicon superlattices, in which no PPC could be induced at temperatures $T < 80$ K.¹¹ This behavior is similar to the effect exhibited by $\text{Zn}_{0.3}\text{Cd}_{0.7}\text{Se}$ mixed crystal here. The authors proposed deep traps of acceptor-like “ AX centers” to be the origin of PPC. In this model, the AX center is analogous to the DX center, yet it implies a thermal barrier against the creation of PPC at low temperatures. However, the high-temperature annealing effects on PPC observed in such a system ruled out the mechanism requiring deep traps.^{12,51}

We think that an important part missing in previously published literature in studying the PPC effect in various bulk materials is the relaxation process of stored charge carriers which contribute to PPC. In fact, from our point of view, whether a theoretical model can thoroughly explain the PPC effect greatly depends on whether or not it can successfully formulate the decay behavior. The DX center of the large lattice relaxation model certainly is not at this stage yet. The macroscopic barrier model predicted a decay formula which is suitable for artificially constructed layered materials. Here, we analyze the PPC decay behavior of previously published data, and attempt to give more information on the nature of PPC in various other materials.

For illustration, in Fig. 8, we reproduce the plots of (a) $\ln[\ln n(0) - \ln n(t)]$ versus $\ln t$ for experimental data obtained for Te-doped $\text{Al}_{0.36}\text{Ga}_{0.64}\text{As}$ material at 63 K (Ref. 2), where n is the electron concentration; (b) $\ln[\ln \sigma(0) - \ln \sigma(t)]$ versus $\ln t$ for data obtained for Si-doped $\text{Al}_{0.3}\text{Ga}_{0.7}\text{As}$ at 85 K (Ref. 52), where σ is the measured conductance, and the dark conductance level has been taken to be 2.5 microsiemens; (c) $\ln[\ln C^2(0) - \ln C^2(t)]$ versus $\ln t$ for pressure-induced PPC effect in Si-doped GaAs at 77.2 K (Ref. 18), where C is the photocapacitance, and the time dependence of C^2 is proportional to the time dependence of bulk carrier concentration; (d) $\ln[\ln I(0) - \ln I(t)]$ versus $\ln t$ for semi-insulating bulk GaAs at 77 K for 9.5 min of light illumination (Ref. 53). PPC exhibited by the $\text{Al}_x\text{Ga}_{1-x}\text{As}$ materials with different dopants and Al concentrations have a similar behavior. The pressure-induced PPC effect in Si-doped GaAs has a much longer relaxation time, however, with a relatively close value of β (=slope of the plots). The semi-insulating bulk GaAs shows quite different behavior, i.e., much smaller values of β and τ . However, the linear behaviors for all of these plots are evident, which indicates that the decay of the photoexcited charge carriers in the above-mentioned materials can be described by the stretched-exponential function. The decay exponents β and the characteristic decay-time constants for materials listed in (a), (b), (c), and (d) are 0.51 and 594 s, 0.5 and 497 s, 0.43 and 282 764 s, and 0.22 and 0.63 s, respectively. The decay kinetics of PPC observed in these materials has not yet been established. The macroscopic barrier model predicates a PPC decay essentially logarithmic in time. The DX center of the large lattice relaxation model predict recombination rates to be governed by monomolecular or possibly bimolecular reaction kinetics.⁸ In fact, it has been suggested by Campbell and Streetman²⁷ that the decay of PPC observed in $\text{Al}_{0.35}\text{Ga}_{0.65}\text{As}$ material can be described by variations of

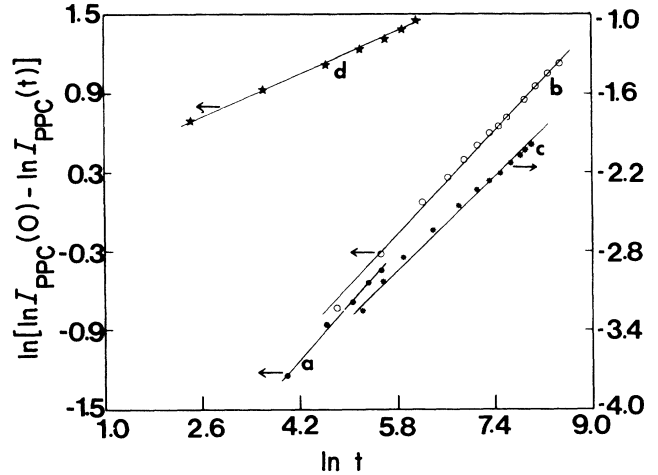


FIG. 8. Plots of (a) $\ln[\ln n(0) - \ln n(t)]$ vs $\ln t$ for experimental data obtained for Te-doped $\text{Al}_{0.36}\text{Ga}_{0.64}\text{As}$ material at 63 K (Ref. 2), where n is the electron concentration; (b) $\ln[\ln \sigma(0) - \ln \sigma(t)]$ vs $\ln t$ for data obtained for Si-doped $\text{Al}_{0.3}\text{Ga}_{0.7}\text{As}$ at 85 K (Ref. 52), where σ is the measured conductance, and the dark conductance level has been taken to be 2.5 microsiemens; (c) $\ln[\ln C^2(0) - \ln C^2(t)]$ vs $\ln t$ for pressure-induced PPC effect in Si-doped GaAs at 77.2 K (Ref. 18), where C is the photocapacitance, and the time dependence of C^2 is proportional to the time dependence of bulk carrier concentration; (d) $\ln[\ln I(0) - \ln I(t)]$ versus $\ln t$ for semi-insulating bulk GaAs at 77 K for 9.5 min of light illumination (Ref. 53). The units of time for all the plots are in s. The solid lines are a guide to the eyes.

has been taken to be 2.5 microsiemens; (c) $\ln[\ln C^2(0) - \ln C^2(t)]$ versus $\ln t$ for the pressure-induced PPC effect in Si-doped GaAs at 77.2 K (Ref. 18), where C is the photocapacitance, and the time dependence of C^2 is proportional to the time dependence of bulk carrier concentration; (d) $\ln[\ln I(0) - \ln I(t)]$ versus $\ln t$ for semi-insulating bulk GaAs at 77 K for 9.5 min of light illumination (Ref. 53). PPC exhibited by the $\text{Al}_x\text{Ga}_{1-x}\text{As}$ materials with different dopants and Al concentrations have a similar behavior. The pressure-induced PPC effect in Si-doped GaAs has a much longer relaxation time, however, with a relatively close value of β (=slope of the plots). The semi-insulating bulk GaAs shows quite different behavior, i.e., much smaller values of β and τ . However, the linear behaviors for all of these plots are evident, which indicates that the decay of the photoexcited charge carriers in the above-mentioned materials can be described by the stretched-exponential function. The decay exponents β and the characteristic decay-time constants for materials listed in (a), (b), (c), and (d) are 0.51 and 594 s, 0.5 and 497 s, 0.43 and 282 764 s, and 0.22 and 0.63 s, respectively. The decay kinetics of PPC observed in these materials has not yet been established. The macroscopic barrier model predicates a PPC decay essentially logarithmic in time. The DX center of the large lattice relaxation model predict recombination rates to be governed by monomolecular or possibly bimolecular reaction kinetics.⁸ In fact, it has been suggested by Campbell and Streetman²⁷ that the decay of PPC observed in $\text{Al}_{0.35}\text{Ga}_{0.65}\text{As}$ material can be described by variations of

stretched-exponential forms. Observation of stretched-exponential decay of PPC in various materials suggests that the random local-potential fluctuations induced by compositional fluctuations or impurity distributions may play an important role for the relaxation of the photoexcited charge carriers except for semi-insulating bulk GaAs because much smaller values of τ and β were observed. The physical meaning of stretched-exponential decay of PPC in semi-insulating bulk GaAs is not clear and the decay kinetics in this material remains to be investigated. We should point out that we also fit the decay of PPC observed in artificially constructed layered materials at low temperatures^{8,54} to the stretched exponential. We found that there are multiple values of β and τ which give a least-squares fit. However, small variation in β result in several orders of magnitude change in τ . Thus such a fit yields no physical significance. This implies that PPC observed in artificially constructed layered materials does not exhibit any characteristic phenomena of disordered systems, and is caused by the spatial separation of the photogenerated charge carrier by the built-in macroscopic barrier due to band bending at the hetero-junction interface.

As temperature increases, the decay behavior of PPC observed in the $\text{Al}_x\text{Ga}_{1-x}\text{As}$ system deviates from the stretched-exponential form, which is similar to the PPC behavior in $\text{Zn}_{0.3}\text{Cd}_{0.7}\text{Se}$ mixed crystal. However, the decay of PPC observed in various other materials at higher temperatures obeys the power law. In Fig. 9, we reproduce the plots of (a) $\ln n(t)$ versus $\ln t$ for Te-doped $\text{Al}_{0.3}\text{Ga}_{0.7}\text{As}$ at 76 K (Ref. 2); (b) $\ln C^2(t)$ versus $\ln t$ for Si-doped GaAs under pressure at 91 K (Ref. 18); (c) $\ln I(t)$ versus $\ln t$ for modulation doped amorphous silicon (*a*-Si) superlattice at 300 K (Ref. 11). The PPC-decay curves of different materials have been rescaled for pre-

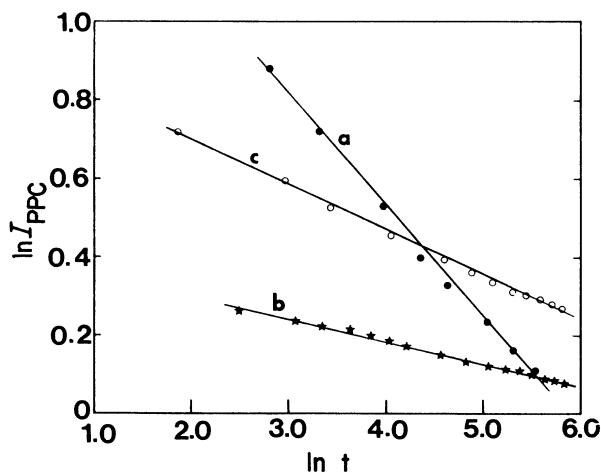


FIG. 9. Plots of (a) $\ln n(t)$ vs $\ln t$ for Te-doped $\text{Al}_{0.3}\text{Ga}_{0.7}\text{As}$ at 76 K (Ref. 2); (b) $\ln C^2(t)$ vs $\ln t$ for Si-doped GaAs under pressure at 91 K (Ref. 18); (c) $\ln I(t)$ vs $\ln t$ for the modulation doped amorphous silicon superlattice at 300 K (Ref. 11). The units of time for all the plots are in s. The solid lines are a guide to the eyes.

sentation. The low-temperature data for the modulation doped silicon superlattice is not available. The PPC effect observed in doping-modulated *a*-Si superlattice may be a consequence of the random potential fluctuations induced by compensation doping. It is known that for a large degree of compensation the charge carriers are distributed highly inhomogeneously in localized regions of impurity potential relief.²⁹ All the plots in Fig. 9 depict linear behaviors, which demonstrates that the decay of PPC observed in various materials at higher temperatures obeys the power law. The link between the stretched-exponential and the power-law relaxation has not yet been established. However, the dynamics of a microscopic model for continuous-time random walk have been investigated most recently,⁵⁵ in which case the Walker's motion includes the hopping of a localized particle and a spin (or dipole) flip. The waiting-time distribution $Q(t)$ derived from the time-dependent perturbation theory has an expression $Q(t) = \exp(-at^{(a-\beta)})$ for $0 \leq \beta < 2$ and $Q(t) \approx t^{-\alpha}$ for $\beta = 2$. The authors pointed out that applications of their theory include dispersion diffusion, the transient drift of hopping controlled light excitation in *a*-Si:H, and the thermoremanent magnetization on spin glasses. Based on such theoretical calculations, the coexistence of the stretched-exponential and the power-law relaxation at different temperatures in disordered systems is not a surprising observation.

Some published decay data of PPC cannot be fitted by either the stretched-exponential or the power-law decay. However, in most of these cases, a clear PC effect is presented. Therefore, these results are not contrary to our interpretations. Other supporting evidence for the random local-potential fluctuation model is the observation of the PPC effect in compensated crystalline bulk CdS single crystal, in which a sharp transition in PPC occurs near 1.5 K.⁵⁶ The transition temperature occurring at lower temperature in CdS may be interpreted as being due to the fact that the degree of the potential fluctuation due to the compensation is much lower in the CdS single crystals than that in mixed crystal alloys. On the other hand, for mixed crystals with smaller compositional fluctuations, the transition temperature should occur at lower temperatures. This interpretation is confirmed very recently by our experimental results obtained on a higher-quality $\text{CdS}_{0.5}\text{Se}_{0.5}$ mixed crystal, in which a similar phase transition takes place near 15 K.⁵⁷

V. CONCLUSION

PPC has been investigated in a $\text{Zn}_{0.3}\text{Cd}_{0.7}\text{Se}$ mixed crystal. A phase transition corresponding to electrons activated from localized to percolation states has been discovered. The PPC relaxation follows the stretched-exponential-decay behavior at low temperatures. Based on the experimental observations, we interpreted the observed PPC in terms of the random local-potential fluctuations induced by the compositional fluctuations. The correlation between the critical temperature T_C , and the fluctuation parameter σ of the sample has been theoretically established. The PPC-decay behavior for previously published data on various materials is also analyzed. We

found that at low temperatures, the decays of PPC exhibited by Te- and Si-doped $\text{Al}_x\text{Ga}_{1-x}\text{Ga}$ and Si-doped GaAs under pressure can be described by the stretched exponential. At higher temperatures, the decay of PPC in these various materials follows the power law. Since the stretched-exponential decay and critical behavior are characteristic phenomena of disordered systems, we think that the random local-potential fluctuations induced either by compositional fluctuations or by impurity

distributions may also cause the PPC effect in other systems.

ACKNOWLEDGMENTS

We would like to thank Mr. S. X. Huang for his assistance in searching the literature for previously published data.

- ¹M. K. Sheinkman and A. Ya. Shik, *Fiz. Tekh. Poluprovodn.* **10**, 209 (1976) [*Sov. Phys.—Semocond.* **10**, 128 (1976)].
- ²R. J. Nelson, *Appl. Phys. Lett.* **31**, 351 (1977).
- ³D. V. Lang and R. A. Logan, *Phys. Rev. Lett.* **39**, 635 (1977).
- ⁴D. V. Lang, R. A. Logan, and M. Joros, *Phys. Rev. B* **19**, 1015 (1979).
- ⁵D. M. Collins, Dan E. Mars, B. Fischer, and C. Kocot, *J. Appl. Phys.* **54**, 857 (1983).
- ⁶M. Mizuta and K. Mori, *Phys. Rev. B* **37**, 1043 (1988).
- ⁷H. J. Queisser and D. E. Theodorou, *Phys. Rev. Lett.* **43**, 401 (1979).
- ⁸H. J. Queisser and D. E. Theodorou, *Phys. Rev. B* **33**, 4027 (1986).
- ⁹D. E. Theodorou and H. J. Queisser, *J. Appl. Phys.* **23**, 121 (1980).
- ¹⁰J. Kakalios and H. Fritzsche, *Phys. Rev. Lett.* **53**, 1602 (1984).
- ¹¹M. Hundgaussen and L. Ley, *Phys. Rev. B* **32**, 6655 (1985).
- ¹²S. H. Choi, B. S. Yoo, and C. Lee, *Phys. Rev. B* **36**, 6479 (1987).
- ¹³H. X. Jiang and J. Y. Lin, *Phys. Rev. B* **40**, 10025 (1989).
- ¹⁴J. Y. Lin, S. X. Huang, L. Q. Zu, E. X. Ping, and H. X. Jiang, *J. Lumin.* (to be published).
- ¹⁵M. I. Nathan, *Solid State Electron.* **29**, 167 (1986).
- ¹⁶H. J. Stormer, R. Dingle, A. C. Gossard, W. W. Wiegmann, and M. D. Sturge, *Solid State Commun.* **29**, 705 (1974).
- ¹⁷D. E. Theodorou, H. J. Queisser, and E. Bauser, *Appl. Phys. Lett.* **41**, 628 (1982).
- ¹⁸M. F. Li, P. Y. Yu, E. R. Weber, and W. Hansen, *Phys. Rev. B* **36**, 4531 (1987).
- ¹⁹W. Shen, P. Y. Yu, M. F. Li, W. L. Hansen, and E. Bauser, *Phys. Rev. B* **40**, 7831 (1989).
- ²⁰D. K. Maude, J. C. Portal, L. Dmowski, T. Foster, L. Eaves, M. Nathan, M. Heiblum, J. J. Harris, and R. B. Beall, *Phys. Rev. Lett.* **59**, 815 (1987).
- ²¹D. J. Chadi and K. J. Chang, *Phys. Rev. Lett.* **57**, 873 (1988).
- ²²D. J. Chadi and K. J. Chang, *Phys. Rev. B* **39**, 10063 (1989).
- ²³M. F. Li, Y. B. Jia, P. Y. Yu, J. Zhou, and J. L. Gao, *Phys. Rev. B* **40**, 1430 (1989).
- ²⁴K. A. Hkachatryan, D. D. Awshalom, J. R. Rozen, and E. R. Weber, *Phys. Rev. Lett.* **63**, 1311 (1989).
- ²⁵P. M. Mooney, N. S. Caswell, and S. L. Wright, *J. Appl. Phys.* **62**, 4786 (1987).
- ²⁶J. C. Bourgoin, S. L. Feng, and H. J. von Bardeleben, *Appl. Phys. Lett.* **53**, 1841 (1988).
- ²⁷A. C. Campbell and B. G. Streetman, *Appl. Phys. Lett.* **54**, 445 (1989).
- ²⁸S. Zukotynski and P. C. H. Ng, *Phys. Rev. Lett.* **59**, 2810 (1987).
- ²⁹B. I. Shklovskii and A. L. Efros, *Zh. Eksp. Teor. Fiz.* **60**, 867 (1971) [*Sov. Phys.—JETP* **33**, 468 (1971)]; **34**, 435 (1972) [**34**, 435 (1972)]; **62**, 1156 (1972) [**35**, 610 (1972)].
- ³⁰S. M. Ryvkin and I. S. Shlimak, *Phys. Status Solidi A* **16**, 515 (1973).
- ³¹A. F. S. Penna, J. Shah, T. Y. Chang, and M. S. Burroughs, *Solid State Commun.* **51**, 425 (1984).
- ³²P. Blood and A. D. C. Grassie, *J. Appl. Phys.* **56**, 1866 (1984).
- ³³J. A. Kash, A. Ron, and E. Cohen, *Phys. Rev. B* **28**, 6147 (1983).
- ³⁴M. Ya. Valakh, M. P. Lisitsa, G. S. Pekar, G. N. Polysskii, V. I. Sidorenko, and A. M. Yaremko, *Phys. Status Solidi B* **113**, 635 (1982).
- ³⁵A. Blumen, J. Klafler, and G. Zumofen, in *Optical Spectroscopy of Glasses*, edited by I. Zschokke (Reidel, Dordrecht, 1986), pp. 199–265.
- ³⁶G. Kriza and G. Mihaly, *Phys. Rev. Lett.* **56**, 2529 (1986).
- ³⁷R. V. Chamberlin, G. Mozurkewich, and R. Orbach, *Phys. Rev. Lett.* **52**, 867 (1984).
- ³⁸J. Kakalios, R. A. Street, and W. B. Jackson, *Phys. Rev. Lett.* **59**, 1037 (1987).
- ³⁹R. G. Palmer, D. L. Stein, E. Abrahams, and P. W. Anderson, *Phys. Rev. Lett.* **53**, 958 (1984).
- ⁴⁰See, for example, P. Dutta and P. M. Horn, *Rev. Mod. Phys.* **53**, 497 (1981).
- ⁴¹D. G. Thomas, J. J. Hopfield, and W. M. Augustyniak, *Phys. Rev.* **140**, A202 (1965).
- ⁴²H. X. Jiang, *Phys. Rev. B* **37**, 4126 (1988).
- ⁴³J. R. Eggert, *Phys. Rev. B* **29**, 6669 (1984).
- ⁴⁴L. E. Reichl, *A Modern Course in Statistical Physics* (University of Texas, Austin, 1980).
- ⁴⁵B. I. Shklovskii and A. L. Efros, in *Electronic Properties of Doped Semiconductors*, Vol. 45 of *Springer Series in Solid-State Sciences*, edited by M. Cardona, P. Fulde, and H. J. Queisser (Springer-Verlag, New York, 1984), p. 297.
- ⁴⁶L. Samel and Y. Brada, *Phys. Rev. B* **37**, 4671 (1988).
- ⁴⁷B. R. Nag, in *Electron Transport in Compound Semiconductors*, Vol. 11 of *Springer Series in Solid-State Sciences*, edited by M. Cardona, P. Fulde, and H. J. Queisser (Springer-Verlag, New York, 1984).
- ⁴⁸A. Kastalsky and J. C. M. Hwuang, *Appl. Phys. Lett.* **44**, 333 (1984).
- ⁴⁹L. X. He, K. P. Martin, and R. J. Higgins, *Phys. Rev. B* **36**, 6508 (1987).
- ⁵⁰D. M. Collins, D. E. Mars, B. Fisher, and C. Kocot, *J. Appl. Phys.* **54**, 857 (1983).
- ⁵¹Suk-Ho Choi, G. L. Park, and C. Lee, *Solid State Commun.* **59**, 177 (1986).
- ⁵²T. W. Dowson and J. F. Wager, in *Chemistry and Defects in Semiconductor Heterostructures*, Vol. 148 of *Proceeding of the*

- Materials Research Society Symposia*, edited by M. Kawabe, T. D. Sands, E. R. Weber, and R. S. Williams (MRS, Pittsburgh, 1989), pp. 445–450.
- ⁵³J. Jiménez, P. Hernández, J. A. de Saja, and J. Bonafé, *Phys. Rev. B* **35**, 3832 (1987).
- ⁵⁴H. J. Queisser, *Phys. Rev. Lett.* **54**, 234 (1985).
- ⁵⁵Fui-Sui Liu and Wen Chao, *Phys. Rev. B* **40**, 7091 (1989).
- ⁵⁶D. Baum, J. Y. Lin, and A. Honig, *Bull. Am. Phys.* **33**, 301 (1988).
- ⁵⁷J. Y. Lin, S. X. Huang, and H. X. Jiang (unpublished).